Backbone Flexibility, Conformational Change, and Catalysis in a Phosphohexomutase from *Pseudomonas aeruginosa*[†,‡]

Andrew M. Schramm,[§] Ritcha Mehra-Chaudhary,[§] Cristina M. Furdui,*[,||] and Lesa J. Beamer*[,§]

Departments of Biochemistry and Chemistry, University of Missouri, Columbia, Missouri 65211, and Department of Internal Medicine, Wake Forest University Health Sciences, Winston-Salem, North Carolina 27157

Received March 26, 2008; Revised Manuscript Received June 27, 2008

ABSTRACT: The enzyme phosphomannomutase/phosphoglucomutase (PMM/PGM) from the bacterium *Pseudomonas aeruginosa* is involved in the biosynthesis of several complex carbohydrates, including alginate, lipopolysaccharide, and rhamnolipid. Previous structural studies of this protein have shown that binding of substrates produces a rotation of the C-terminal domain, changing the active site from an open cleft in the apoenzyme into a deep, solvent inaccessible pocket where phosphoryl transfer takes place. We report herein site-directed mutagenesis, kinetic, and structural studies in examining the role of residues in the hinge between domains 3 and 4, as well as residues that participate in enzyme−substrate contacts and help form the multidomain "lid" of the active site. We find that the backbone flexibility of residues in the hinge region (e.g., mutation of proline to glycine/alanine) affects the efficiency of the reaction, decreasing k_{cat} by ∼10-fold and increasing K_m by ∼2-fold. Moreover, thermodynamic analyses show that these changes are due primarily to entropic effects, consistent with an increase in the flexibility of the polypeptide backbone leading to a decreased probability of forming a catalytically productive active site. These results for the hinge residues contrast with those for mutants in the active site of the enzyme, which have profound effects on enzyme kinetics (10^2-10^3-fold decrease in k_{cat}/K_m) and also show substantial differences in their thermodynamic parameters relative to those of the wild-type (WT) enzyme. These studies support the concept that polypeptide flexibility in protein hinges may evolve to optimize and tune reaction rates.

The enzyme PMM/PGM[1] plays a key role in the production of carbohydrates by *Pseudomonas aeruginosa*, an opportunistic human pathogen. Three of these molecules are alginate, a secreted exopolysaccharide; lipopolysaccharide, the major component of the outer membrane of the bacterium; and rhamnolipid, a surfactant involved in biofilm maintenance (*1, 2*). Several studies, including animal models of infection, have shown that *P. aeruginosa* strains lacking PMM/PGM exhibit slower growth rates and decreased virulence and are more easily cleared by the host immune system (*3, 4*). Hence, PMM/PGM is an attractive target for the development of clinical inhibitors, which could have utility in the treatment of antibiotic resistant infections by this organism.

PMM/PGM participates in the early stages of carbohydrate biosynthesis, catalyzing the reversible conversion of 1- to 6-phosphosugars via a bisphosphorylated sugar intermediate (*5*). It can utilize both glucose- and mannose-based substrates with equal efficiency (*6*). The reaction entails two phosphoryl transfer reactions: first from a phosphoserine residue on the enzyme to substrate and second from the reaction intermediate (e.g., glucose 1,6-bisphosphate or G16P) back to the enzyme. Previous studies of PMM/PGM have shown that G16P must undergo an ∼180° reorientation between the two phosphoryl transfer steps and that this occurs without dissociation of the intermediate from the enzyme (*7, 8*). Thus, the PMM/PGM reaction may be considered a simple example of processivity, as defined by multiple rounds of catalysis without release of substrate (*9*).

Several lines of evidence have suggested that conformational change plays a critical role in the reaction of PMM/PGM. Structural studies of the enzyme, as both apoprotein and in complex with its substrates and products (*8, 10*), show that an interdomain rotation of the enzyme occurs upon substrate binding, which is necessary to create a high-affinity ligand binding site and position the substrate appropriately for catalysis. In addition, steady-state and pre-steady-state kinetics investigations have substantiated the critical, rate-limiting role of the nonchemical steps of the PMM/PGM reaction (i.e., ligand binding and release and/or conforma-

[†] Supported by a grant from the MU Children's Miracle Network to L.J.B. The Advanced Light Source is supported by the Director, Office of Science, Office of Basic Energy Sciences, of the U.S. Department of Energy under Contract DE-AC02-05CH11231.

[‡] The structures of the P368G mutant and its complex with substrate have been deposited in the Protein Data Bank (PDB) as entries 3C04 and 3BKQ, respectively.

* To whom correspondence should be addressed. L.J.B.: telephone, (573) 882-6072; fax, (573) 884-4812; e-mail, beamerl@missouri.edu. C.M.F.: telephone, (336) 716-2697; fax, (336) 716-1214; e-mail, cfurdui@wfubmc.edu.

[§] University of Missouri.

[||] Wake Forest University Health Sciences.

[1] Abbreviations: PMM/PGM, phosphomannomutase/phosphoglucomutase; DTT, dithiothreitol; MOPS, 3-(*N*-morpholino)propanesulfonic acid; rmsd, root-mean-square deviation; EDTA, ethylenediaminetetraacetate; NAD^+, nicotinamide adenine dinucleotide (oxidized form); NADH, nicotinamide adenine dinucleotide (reduced form); G1P, glucose 1-phosphate; G16P, glucose 1,6-bisphosphate; WT, wild-type.

10.1021/bi8005219 CCC: $40.75
Published on Web 08/09/2008

tional change) (*7*). Moreover, structural studies of enzyme−intermediate complexes have shown that the required reorientation of the intermediate cannot occur without opening of the active site cleft (*9*). PMM/PGM therefore offers an opportunity to study conformational change in mechanistically unique enzyme system where the nonchemical steps of the reaction are rate-limiting.

The interdomain rotation of PMM/PGM is quite distinct from the hinge motions of small loops that have been studied well in many enzymes, including adenylate kinase (*11*), DHFR (*12*), mandelate racemase (*13*), *S*-adenosylmethionine synthetase (*14*), and TIM (*15–21*). In the case of TIM, mutational studies have been paired with kinetic and NMR experiments in attempts to elucidate the importance of backbone flexibility in the active site loop (*16, 20, 21*). These elegant studies have shown that an increase in the number of conformational accessible states is correlated with a reduction in enzyme activity and led to the proposal that structural rigidity of the hinges in TIM is essential to limit the number of effective conformational states and focus the motions of the active site loops.

To study the effect of increased backbone/hinge flexibility on the PMM/PGM reaction and its interdomain rotation, we have introduced site-directed mutations of several key residues in the hinge region and the neighboring interdomain interface. In addition, two active site mutants were characterized to compare the effects of changes on enzyme−substrate interactions with the potential conformational impact of mutations in the hinge region. In the work presented here, we describe structural, kinetic, and thermodynamic characterization of these mutants in an effort to improve our understanding of backbone flexibility and conformational change in the PMM/PGM reaction and the role of hinges in enzyme catalysis.

EXPERIMENTAL PROCEDURES

Materials. G1P, G16P, and glucose-6-phosphate dehydrogenase from *Leuconostoc mesenteroides* were obtained from Sigma.

Protein Expression, Purification, and Site-Directed Mutagenesis. WT and mutant *P. aeruginosa* PMM/PGM proteins were purified via a $(His)_6$ tag at the N-terminus as previously described (*22*). Purified proteins were dialyzed overnight into 10 mM MOPS (pH 7.4) and 1 mM EDTA to remove foreign metals, with a final dialysis against 1 mM $MgCl_2$ and 10 mM MOPS. After dialysis, proteins were incubated with 2 μM G16P at room temperature for 1 h to ensure full phosphorylation of the active site serine; excess G16P was subsequently removed by dialysis. Site-directed mutants of PMM/PGM were constructed using the QuikChange mutagenesis kit (Stratagene) and mutations verified by automated DNA sequencing.

Steady-State Kinetic Studies. The activity of each mutant protein was quantitated by measuring the PGM activity in the direction of glucose 6-phosphate formation, using a coupled assay with glucose-6-phosphate dehydrogenase as previously described (*6*), with several minor modifications. Reactions were conducted at 25 °C in 50 mM MOPS (pH 7.4) with 1 mM DTT, 1.5 mM $MgSO_4$, 1 μM G16P, and 0.9 mM NAD^+. The substrate (G1P) concentration was varied from 1 to 200 μM; the enzyme concentration depended on activity (5 μg/mL for WT and up to 200 μg/mL for the Y17A and E325A mutants). The reaction was monitored by measuring the rate of production of NADH, based on its absorbance at 340 nm. The data were fitted to the Michaelis−Menten equation to determine the reaction rate (k_{cat}, s^{-1}) and the Michaelis−Menten constant (K_m, μM).

Temperature Dependence Studies. The temperature dependence of the PMM/PGM reaction was determined using the assay described above, but at a single substrate concentration of 50 μM G1P. Assays were conducted at temperatures ranging from 4 to 40 °C in increments of no more than 5 °C. As WT PMM/PGM exhibited a decrease in activity between 35 and 40 °C, temperatures above 35 °C were not tested for the mutant enzymes. The temperature dependence of the reaction rate constants for the WT and mutant PMM/PGM was analyzed first with the Arrhenius equation to extract the energy of activation, E_a. The E_a parameter was determined from the slope ($-E_a/R$) of the linear plot of ln k versus $1/T$. The activation enthalpy ($\Delta H^{\ddagger}_{298}$) was calculated as $E_a - RT$. The free energy of activation ($\Delta G^{\ddagger}_{298}$) was calculated as $RT[\ln(k_BT/h) - \ln(k)]$, where $R = 1.9872$ cal mol^{-1} K^{-1}, k_B is the Boltzmann constant (1.38066×10^{-23} J K^{-1}), and h is Planck's constant (6.62608×10^{-34} J s). The activation entropy ($\Delta S^{\ddagger}_{298}$) was then calculated as $(\Delta H^{\ddagger}_{298} - \Delta G^{\ddagger}_{298})/T$ (*23, 24*).

Crystallization and Structure Determination. The P368G hinge mutant was selected for structural analysis and expressed in *Escherichia coli* using the pET3a vector, which lacks an N-terminal His tag (the His tag is not compatible with crystallization). The protein was purified and crystallized as previously described for the WT enzyme (*6, 10, 25*). To form complexes with substrate, quick soaks of crystals were conducted in solutions of 100 mM G1P and 75% PEG 4000, following a protocol developed previously (*8*). X-ray diffraction data were collected on crystals of both the apoprotein mutant (Rigaku RU H3R rotating anode) and a complex of the mutant with G1P (ALS beamline 4.2.2) under cryocooling conditions. A summary of data collection statistics is presented in Table 1.

Data were processed with DENZO (apo-P368G) or d*Trek (P368G complex) (*26, 27*), and refinement was performed with REFMAC 5.0 (*28*). For the apo-P368G crystals, the starting model for refinement was that of WT apo-PMM/PGM (PDB entry 1K35) without water molecules, and for the P368G complex with substrate, the starting model was the corresponding substrate complex for the WT enzyme (PDB entry 1P5G), without ligands or water molecules. Both structures were refined to convergence through iterative cycles of refinement and manual rebuilding with Coot (*29*). The progress of the refinement was monitored by following R_{free}; 5% of each data set was set aside for cross validation prior to refinement. Water molecules were placed automatically with COOT in peaks $>3.0\sigma$ in $F_o - F_c$ maps and within reasonable hydrogen bonding distance of oxygen or nitrogen atoms. The final models (Table 1) contain the following heteroatoms: phosphoserine 108, Zn^{2+}, and waters.

Occupancy, B Factor, and Other Analyses. The TLS contribution to the protein *B* factors was modeled with domains 1−3 and 4 of the enzyme as separate bodies. The occupancy for all atoms except side chains modeled in alternate conformations is 1.0. For the per residue *B* factor analysis of the protein, the TLS contribution to the *B* factors

Table 1: Crystallographic Data for the P368G Mutant of PMM/PGM

	apo-P368G	P368G−G1P
Data Collection		
X-ray source	home	MBC 4.2.2
space group	$P2_12_12_1$	$P2_12_12_1$
unit cell dimensions (Å)	$a = 70.60$	$a = 70.61$
	$b = 72.25$	$b = 74.72$
	$c = 92.78$	$c = 86.93$
λ (Å)	1.54	1.000
resolution (Å)	50.00−2.2	44.20−2.05
outermost shell	2.20−2.25	2.12−2.05
no. of unique reflections	23903	29408
redundancy	3.6	6.7
R_{merge} (%)	9.5 (46.6)	13.2 (49.1)
I/σ	13.9 (2.0)	7.2 (3.1)
completeness (%)	96.5 (92.5)	99.6 (99.2)
Refinement		
resolution (Å)	50.00−2.2	44.20−2.05
R_{work},[a] R_{free}[b]	17.6, 22.1	21.8, 24.9
no. of non-H atoms	3594	3679
no. of waters	141	208
B value from Wilson plot (Å^2)	36.0	27.3
$\langle B \rangle$ (Å^2)		
protein atoms	32.4	29.4
waters	35.4	33.4
ligands	−	73.0
rmsd for bonds (Å), angles (deg)	0.012, 1.4	0.012, 1.4
Ramachandran (%)	95.6, 3.1[c]	95.6, 3.5[c]

[a] $R_{work} = \sum|F_o - F_c|/\sum|F_c|$, where F_o and F_c are observed and calculated structure factors, respectively. [b] R_{free} is the R factor calculated from 5% of the reflections not included in refinement. No σ cutoff of the data was used. [c] Most favored, allowed regions.

was first removed by performing an additional round of refinement on the final model, without including the TLS option in REFMAC. As the B factor for the G1P ligand in the P368G complex was rather high at full occupancy (Table 1), several trial refinements with lower occupancies were conducted, to determine the occupancy of the ligand where its average B factor would be similar to those of the enzyme residues that interact with the ligand. This approach estimates the ligand occupancy to be between 0.5 and 0.6, despite its presence at 100 mM in the crystal soaks. There is no indication that the enzyme is not 100% in the ligand-bound state, based on the B factor analysis of the protein (see Results) and the previously characterized, distinct change in the unit cell upon formation of the complex for PMM/PGM (*8*), which is also seen with the mutant (Table 1).

Solvent accessible surfaces were calculated with NACCESS (*30*); domain interfaces and gap indices were calculated with the Protein-Protein interaction server (*31*), and rmsd calculations were conducted with SUPERPOSE (*32*). Structural figures were made with Pymol (*33*). Sequence alignments were carried out with ClustalW (*34*), and the figure was produced with JalView (*35*).

RESULTS

Structural Context of the Interdomain Rotation. In previous studies, we have characterized a number of distinct structures of *P. aeruginosa* PMM/PGM at resolutions ranging from 1.6 to 2.2 Å (*8–10, 36*). These include structures of the apoprotein (WT and S108A mutant, PDB entries 1K35 and 1K2Y, respectively) and four enzyme−substrate complexes with G1P, glucose 6-phosphate, mannose 1-phosphate, and mannose 6-phosphate (1P5D, 1P5G, 1PCJ, and 1PCM, respectively). (Since the PMM/PGM reaction is highly reversible, the 1-phosphosugar and 6-phosphosugar species can be termed as either substrate or product; we use substrate for both herein.) Structural comparisons of the apoenzyme and enzyme−substrate complexes show that an ~10° rotation of the C-terminal domain (hereafter called domain 4) occurs upon substrate binding (*8*). The interdomain rotation reduces the volume and solvent accessibility of the active site and also creates an interface between domains 1 and 4 of the protein (Figure 1a). This has the effect of forming a "lid" over the active site, creating a deep pocket where substrates bind and phosphoryl transfer can take place. The domain 1−4 interface is necessary to produce the invariant phosphate-binding site (Figure 1b), a conserved cluster of residues critical for substrate interactions in all four complexes (*8*).

The rotation of domain 4 is produced by a hinge-type movement in a linker region (residues 367−369) between domains 3 and 4 (*8*). The hinge region is far from the active site (nearly 30 Å to the active site phosphoserine) and thus is not directly involved in contacts with bound ligand or phosphoryl transfer. Multiple-sequence alignments reveal a proline residue in the hinge, P368 in *P. aeruginosa* PMM/PGM, which is highly conserved in the enzyme family (see Figure S1 of the Supporting Information). Moreover, inspection of the hinge region in the PMM/PGM structures shows that several residues in this area vary their structural roles depending on whether the protein is in its "open" apo state or in the "closed" enzyme−substrate complex. For example, in three of the four enzyme−substrate complexes, the side chain of hinge residue S369 interacts with the side chain of R262, a residue in domain 3 (Figure 1c). However, this contact is not seen in an apoenzyme structure (1K2Y, a model for the dephosphorylated form of the enzyme), where the active site of the enzyme exhibits its most open conformation. These and other structural differences between the apoproteins and enzyme−substrate complexes further supported the idea that the hinge residues (and their associated interactions) could be relevant to the conformational changes of PMM/PGM necessary for catalysis.

Structural Consequences of the P368G Mutation in the Hinge Region. To investigate the structural impact of increased backbone flexibility in the hinge region of PMM/PGM, the conserved proline residue was changed to a glycine. The P368G mutant was crystallized and its structure determined with and without bound substrate at 2.05 and 2.2 Å resolution, respectively (Table 1). Overall, the structures of both apo-P368G and ligand-bound P368G are similar to those of WT enzyme: the P368G apoprotein has a C_α rmsd of 0.41 Å^2 compared to the WT apoenzyme (1K35); the P368G−G1P complex has a C_α rmsd of 0.51 Å^2 relative to the WT−G1P complex (1P5D). Figure 2 shows the superimposed structures of the apoprotein and enzyme−substrate complexes of P368G and WT PMM/PGM.

Because of the large difference in the backbone flexibility of proline and glycine, the P368G mutant was expected to show the most significant structural changes in the hinge region. Indeed, the substitution of the proline with a glycine produces a large change in the backbone conformation of several residues in the hinge of PMM/PGM (Figure 2b,d and Figure S2 of the Supporting Information). This change is initiated with a nearly 180° difference in the ψ angle of F367; large structural differences are also observed in G368 and

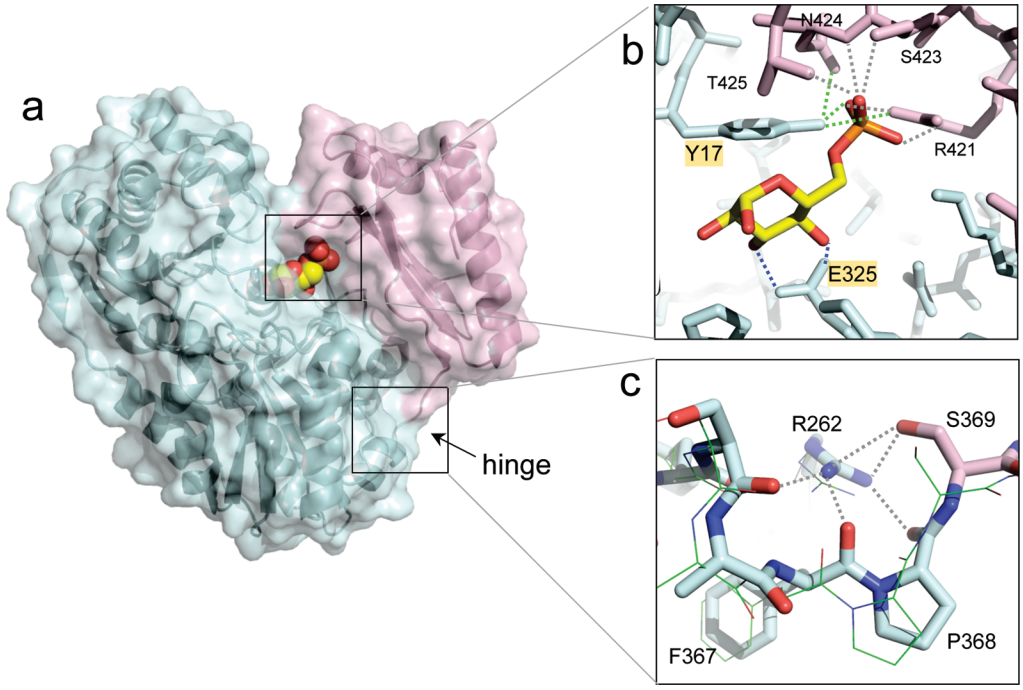

FIGURE 1: (a) Ribbon diagram with the molecular surface of *P. aeruginosa* PMM/PGM in complex with its substrate glucose 6-phosphate (1P5G) (*8*). Domains 1−3 (residues 1−368) are colored cyan; domain 4 (residues 369−463) is colored pink. Glucose 6-phosphate is shown as a space-filling model. The location of the hinge region at the interface of domains 3 and 4 is highlighted with an arrow. (b) Close-up view of Y17 and E325 showing their respective roles in the active site of the enzyme. Glucose 6-phosphate is shown in the same orientation as in panel a. Y17 participates in both enzyme−substrate and protein−protein contacts (green dashed lines), while E325 makes key contacts with the O3 and O4 hydroxyls of the substrate (blue lines). Other enzyme contacts with the phosphate group of the ligand are also shown (gray lines) to highlight the hydrogen bond network surrounding the phosphosugar. (c) Close-up view of residues in the hinge region, showing the network of hydrogen bonds (dashed lines) surrounding R262 (indicated contacts are all ≤3.0 Å). The same region from the apoenzyme is shown with thin lines. Although details vary, a similar network of contacts is also seen in other PMM/PGM enzyme−substrate complexes.

S369. In the apo-P368G structure, the side chain of R289, which is near the hinge region, adopts a new conformation (Figure 2b), resulting in a novel hydrogen bond with the backbone oxygen of F367. The backbone angles of residues following the hinge region (S369 and onward through the chain) are generally very similar to those of the WT enzyme. However, in both the apoenzyme and enzyme−substrate complex, small displacements in parts of the polypeptide backbone of domain 4 are observed (Figure 2a,c), which, although quite subtle, appear to be related to the sequence change in the hinge region.

To assess the potential impact of the P368G mutant on the flexibility and/or disorder of the protein structure, *B* factor analyses of the P368G apoenzyme and enzyme−ligand complex were performed (see Experimental Procedures). These show that that while residues in the hinge tend to have higher than average *B* factors (see Figure S3 of the Supporting Information), they are not significantly greater than those of residues in loops or turns of the protein. Overall, *B* factors for residues in domain 4 do not differ from those in the other domains of the protein. These results are similar to those seen in the structures of WT PMM/PGM, where *B* factors of the hinge residues are a bit above average for the protein (data not shown), indicating that the P368G mutation does not significantly increase the static disorder of the hinge region or domain 4 of the protein in the crystal.

To quantify the cumulative effects of the small structural changes observed in the P368G structures, the interaction surface area between domain 4 and the rest of the enzyme was calculated. In addition, a measure of domain interface complementarity, known as the gap index, was determined (*31*). (The gap index is a small number for highly complementary surfaces; larger numbers indicate less complementarity.) The results of these calculations, for both P368G and WT PMM/PGM, are summarized in Table 2. When compared with data for WT PMM/PGM, these calculations show a higher gap index (by 0.7 unit) for the apoenzyme structure of the P368G mutant. In the presence of bound substrate, both the WT and P368G structures are considerably more compact and show a reduction in the gap index, relative to their respective apoenzyme structures. Notably, the difference in the gap index between the enzyme−substrate complexes and the apoenzyme structures is significantly larger for the P368G mutant than for WT enzyme: a change of 1.3 units for the mutant versus a change of 0.8 unit for WT structures. The interface surface areas for domain 4 (Table 2) are consistent with the gap index data: the P368G mutant has smaller surface interfaces in both the apoenzyme and the enzyme−substrate complex, relative to the WT structures, and also shows a smaller surface area increase upon substrate binding than WT. These calculations are consistent with a potential increase in backbone flexibility for the P368G mutant, resulting in a less complementary interface between domain 4 and the rest of the protein, particularly in the apoenzyme structure. Moreover, the larger difference in the gap index between the apoenzyme and enzyme−substrate complex suggests that the transition between these two structural conformations is more significant for the P368G mutant than for the WT enzyme.

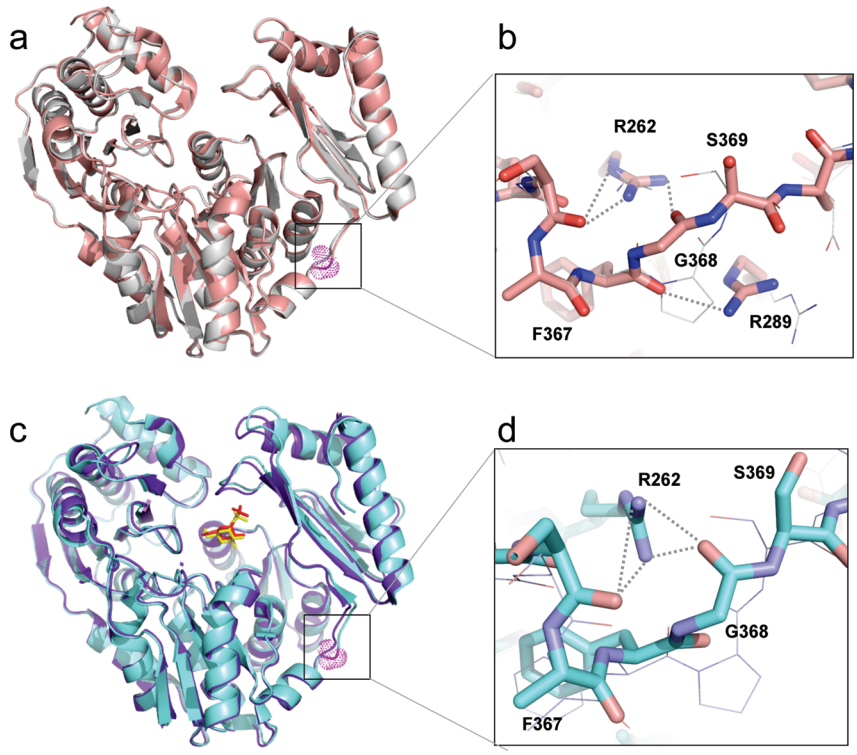

FIGURE 2: Superposition of the P368G and apo-PMM/PGM structures. (a) Ribbon diagram of the apo-P368G (peach) and apo-WT PMM/PGM (gray) structures. The location of the P368G mutation is highlighted with a box and magenta spheres. (b) Close-up view of the hinge in the apo-P368G structure showing the change in backbone conformation for the residues surrounding the mutation. The same region from the apo-WT enzyme (1K35) is shown with thin lines. Potential hydrogen bonds (<3.2 Å) for the P368G structure are indicated with dashed lines. Note the change in conformation of R289 for WT vs mutant structures. (c) Enzyme−G1P complexes for the P368G (cyan) and WT (purple) PMM/PGM with bound glucose 1-phosphate shown as a stick model (yellow for the WT complex, red for the P368G complex). (d) Close-up view of the hinge region in the P369G complex. The WT complex is shown with thin lines. Note the loss of interactions between R262 and S369 relative to Figure 1c.

Table 2: Surface Area of the Interface of Domain 4 and the Rest of the Protein

structure	protein	SA[a] domain interface (Å^2)	% interface nonpolar	gap index[b]
1K35	apo-WT	677.5	44.5	4.2
3C04	apo-P368G	651.5	46.2	4.9
1P5D	WT−G1P	832.9	43.3	3.4
3BKQ	P368G−G1P	780.4	49.3	3.6

[a] SA is surface area. [b] See Results for an explanation of gap index.

Despite the changes in the hinge conformation and domain 4 interface, interactions of residues in the active site of the P368G mutant with substrate are quite similar to those made by WT PMM/PGM. A comparison of the P368G and WT enzyme contacts with G1P (see Table S1 and Figure S4 of the Supporting Information) shows that the same residues are involved and that only small changes in hydrogen bond lengths are observed (i.e., generally <0.5 Å difference). However, there is a 46% increase in the solvent accessible surface area of G1P it is when bound to the P368G mutant, as compared to the WT complex (23.4 Å^2 in WT vs 39.5 Å^2 in P368G). This changes the overall exposed surface area of the ligand from 6.3% (WT) to 9.2% (mutant). The increase in exposed surface area of G1P is most likely due to a slightly more open conformation of the enzyme in the P368G mutant, which can nevertheless maintain enzyme−substrate contacts very similar to those of the WT enzyme. The increased exposed surface area of G1P may contribute to the high *B* factor and/or potential partial occupancy of the ligand (see Table 1 and Experimental Procedures). These might also reflect a lower binding affinity of the mutant for substrate (see the following section) or a greater mobility of the ligand in the active site. An unambiguous assessment of these effects cannot be made due to issues with independently refining *B* factors and occupancies at the moderate 2.05 Å resolution of the structure.

Overall, the structural effects of the P368G mutation, at least as manifested on the static crystallographic structures, appear to originate in the hinge region and propagate as small changes in the domain 4 interface and enzyme−substrate contacts. Among the intriguing possible consequences of these structural changes were alterations in enzyme kinetics due to perturbation of the conformational change required to "close the lid" on the active site of PMM/PGM. The impact of P368G and other hinge and active site mutations on the kinetics and thermodynamic parameters of activation of the PMM/PGM reaction is described in the following sections.

Effect of Hinge and Active Site Mutations on the Kinetics of PMM/PGM. To further study the conformational change and reaction mechanism of PMM/PGM, site-directed mutants were produced in or near the hinge region between domains 3 and 4. Several mutants (P368A and P368G) were designed in an effort to investigate the role of backbone rigidity in the conformational change of the enzyme. Residues S369 and R262 were also chosen for mutagenesis to probe the role of the hinge-associated hydrogen bond network in the conformational change (Figure 1c). To compare the effects of mutations in the hinge with those of residues involved

Table 3: Kinetic Parameters for *P. aeruginosa* PMM/PGM Hinge and Active Site Mutants in the Conversion of Glucose 1-Phosphate to Glucose 6-Phosphate

protein	k_{cat} (s^{-1})	K_m (μM)	k_{cat}/K_m (μM^{-1} s^{-1})	% relative to WT
WT	7.83 ± 0.76	27.2 ± 4.5	0.287868	−
R262A	0.87 ± 0.08	49.1 ± 13.0	0.017719	6.1
P368A	1.02 ± 0.04	35.4 ± 4.5	0.028814	10.0
P368G	1.23 ± 0.15	48.9 ± 16.5	0.025153	8.7
S369A	2.17 ± 0.04	36.6 ± 10.7	0.05929	20.5
R262A/P368G	0.48 ± 0.04	66.7 ± 15.2	0.007196	2.5
Y17A	0.050 ± 0.0050	49.3 ± 12.7	0.001014	0.35
E325A	0.012 ± 0.0005	51.8 ± 6.8	0.000232	0.08

directly in substrate contacts, two additional residues in the active site were also selected for analysis: E325, which is responsible for multiple direct enzyme−substrate contacts, and Y17, which participates in both substrate contacts and the interface between domains 1 and 4 that forms upon substrate binding (Figure 1b) (*8*).

The steady-state kinetic parameters for the PMM/PGM hinge and active site mutants are summarized in Table 3. These data show that mutations of the hinge-associated residues (R262A, P368A, P368G, and S369A) produce generally similar effects: ~10-fold reduction in k_{cat} relative to that of the WT enzyme and a maximum 2-fold increase in K_m. Mutation of S369 to alanine, which was designed to probe the role of hydrogen bond interactions in maintaining hinge rigidity, had the smallest effect on PMM/PGM kinetics. The specificity (k_{cat}/K_m) of the S369A mutant for G1P was only 5-fold lower than that of the WT. Mutation of P368 to glycine or alanine had a greater impact on enzyme kinetics: the k_{cat}/K_m of the P368G/A mutants for G1P was approximately 10% of that of the WT. Consistent with these findings, structural characterization of the P368G mutant (discussed above) shows that mutation of P368 to glycine not only generates a less compact structure (as reflected by the increased gap indices relative to WT) but also disrupts the hydrogen bond interactions between R262 and S369. The R262A mutant, in which the interactions of this side chain with both P368 and S369 are lost, retains only 6% of the specificity of the WT for G1P, even less than the P368G/A or S369A single mutants. Interestingly, the double mutant (R262A/P368G) exhibits a 40-fold reduction in the specificity constant relative to the WT, suggesting a synergistic effect of these residues on the conformational change that controls the PMM/PGM kinetics. The steady-state kinetic parameters of the two active site residues (Y17A and E325A) show increases similar to those of the hinge mutants in K_m when compared to WT PMM/PGM. Unlike the hinge mutants, however, k_{cat} was markedly decreased, resulting in a remarkable 10^2-10^3-fold decrease in k_{cat}/K_m relative to the WT enzyme, even though neither of these residues is directly involved in phosphoryl transfer.

Effect of Hinge and Active Site Mutations on the Thermodynamic Paramaters of Activation of the PMM/PGM Reaction. The consequences of the hinge and active site mutations on the thermodynamics of the PMM/PGM reaction were determined by following the temperature dependence of the reaction rates. Figure 3a shows Arrhenius plots for the reaction rates of WT and mutant PMM/PGM proteins. The activation energy (E_a) for WT and each PMM/PGM mutant was determined from the slope of ln k versus $1/T$ as described in Experimental Procedures. Subsequent data analysis by transition-state theory allowed the determination of the enthalpy, entropy, and free energy of activation for the PMM/PGM reaction ($\Delta H^{\ddagger}$, $\Delta S^{\ddagger}$, and $\Delta G^{\ddagger}$, respectively); details of the analysis are described in Experimental Procedures, and the results are summarized in Figure 3b. In the case of the three non-active site mutants that were characterized, similar effects were seen regardless of the type (P368A vs P368G) or site (the hinge-interacting residue R262 in domain 3 vs P368 located in the hinge) of mutation. Only small decreases in the enthalpy of activation ($\Delta H^{\ddagger}$) were observed. However, a much more negative entropy of activation ($\Delta S^{\ddagger}$) relative to the WT enzyme was found. The thermodynamic parameters of the active site E325A mutant display a similar pattern, but with an even more negative $\Delta S^{\ddagger}$. In contrast, the effects of the Y17A mutation were distinctive, including more positive values for both $\Delta H^{\ddagger}$ and $\Delta S^{\ddagger}$.

DISCUSSION

Our investigation of the steady-state kinetics of the PMM/PGM hinge mutants revealed that, although these residues are >25 Å from the active site, they have a clear affect on catalytic efficiency. Indeed, they have a greater effect than mutation of many previously characterized active site residues (*22*). The quite modest 2-fold increase in K_m for the hinge mutants indicates that their ability to bind substrate is not significantly impaired, with the larger effect being manifested on k_{cat}. Overall, the kinetic results suggest that the flexibility (or lack thereof) of the hinge has a long-range impact on substrate binding and/or the conformational change of the enzyme, each of which is known to be rate-limiting in the multistep PMM/PGM reaction (*7*). Both the inherent flexibility of the polypeptide backbone and changes in the hydrogen bond network of residues in the hinge region appear to be involved in conformational change, as evidenced by the synergistic effects of the R262A/P368A double mutant. The structural characterization of the P368G mutant is consistent with these conclusions from the kinetic analyses.

The thermodynamic analyses of the PMM/PGM hinge mutants provide further insights into a potential role for hinge flexibility in catalysis and support the hypothesis that the degree of conformational flexibility and/or the rate of conformational fluctuations is a critical factor in the catalytic efficiency of PMM/PGM. The more negative $\Delta S^{\ddagger}$ values for the P368A/G and R262A mutants indicate a larger change in entropy between the ground-state and transition-state complex in these proteins as compared with WT PMM/PGM. In each mutant, the slightly favorable decrease in $\Delta H^{\ddagger}$ does not compensate for the unfavorable decrease in $\Delta S^{\ddagger}$. Thus, the reduction in the activity of the hinge mutants appears to be due almost entirely to a higher entropic "penalty" that must be overcome to create a catalytically productive active site. The observed effects on the entropy of activation are consistent with the notion that the hinge mutants have increased flexibility in the protein backbone, potentially leading to an increased number or population of energetically accessible conformations in the ground state, and thereby reducing the probability of adopting the precise conformation required for effective enzyme−substrate interactions and catalysis.

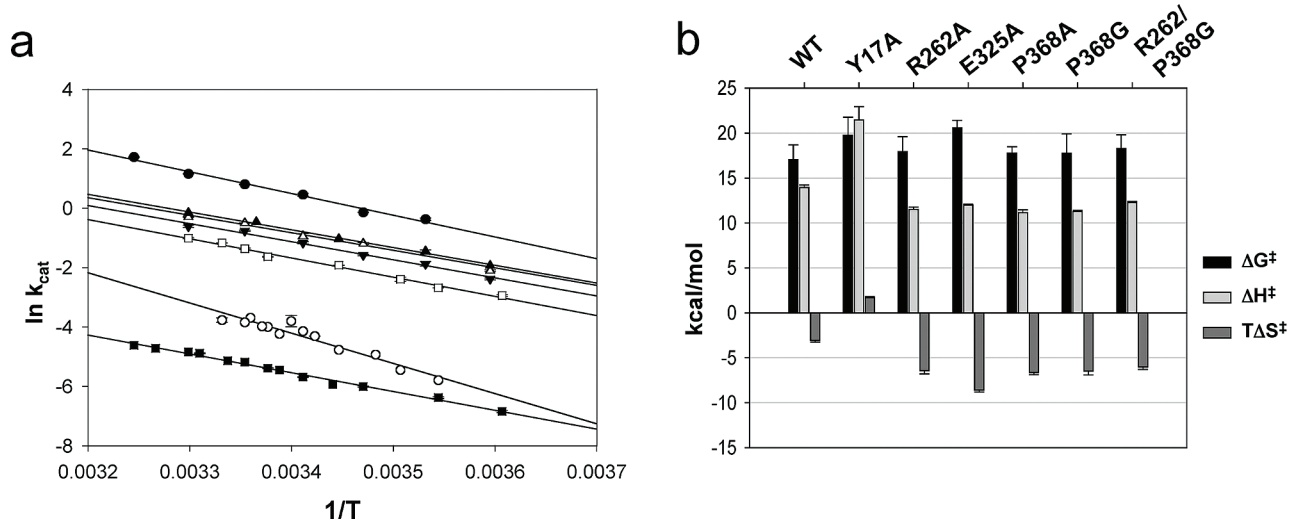

FIGURE 3: (a) Temperature dependence of k_{cat} for WT PMM/PGM (●; $r^2 = 0.98$) and PMM/PGM hinge and active site mutants: P368A (△; $r^2 = 0.97$), P368G (▲; $r^2 = 0.99$), R262A (▼; $r^2 = 0.98$), R262/P368G (□; $r^2 = 0.99$), Y17A (○; $r^2 = 0.93$), and E325A (■; $r^2 = 0.99$). The temperature dependence of k_{cat} for the S369A mutant was not determined. (b) Bar graph comparing the derived thermodynamic parameters for WT PMM/PGM and the mutants in panel a. See Experimental Procedures for details of the analysis. Errors for $\Delta H^{\ddagger}$ were calculated on the basis of the errors in the slope of the Arrhenius plots for WT and each mutant in panel a; errors in $\Delta G^{\ddagger}$ reflect errors in k_{cat} listed in Table 3, and errors for $T\Delta S^{\ddagger}$ were calculated on the basis of the averaged errors for $\Delta H^{\ddagger}$ and $\Delta G^{\ddagger}$. All errors were within ±15%.

In addition to the hinge mutants, we also characterized mutants of two active site residues of PMM/PGM, whose structural roles in enzyme−substrate complexes have been previously well characterized (*8*). Indeed, of the mutants characterized in this study, the E325A protein showed the largest decrease in k_{cat}/K_m (0.08% of that of WT), and also the largest decrease in $\Delta S^{\ddagger}$. This more negative $\Delta S^{\ddagger}$ must derive from a relative decrease in the order of the ground state, a relative increase in the order of the transition state, or some combination thereof. Multiple crystal structures have shown that the E325 side chain makes important enzyme contacts with bound substrate (Figure 1b), and unless solvent molecules compensate for the loss of the side chain in the transition state, it seems unlikely that mutation to alanine would cause an increase in the order of the transition state. Hence, changes in the ground state of E325A seem to be the most likely origin for the more negative $\Delta S^{\ddagger}$.

To gain further insight into the possible effects of mutating this side chain on the order of the ground state, we reviewed the structural roles of E325 in the two apoenzyme structures of PMM/PGM. This analysis is somewhat complicated by the fact that the glutamate side chain is inherently flexible, and indeed, this residue is observed in various conformations in different crystal structures. However, in both 1K35 and 1K2Y, the side chain of E325 makes multiple hydrogen bond interactions, including conserved interactions with the side chain of S327 and two water molecules (Figure 4.) In addition, it interacts with the backbone amide groups of two residues, although the identity of these varies depending on conformation of the side chain observed, making a total of five or six hydrogen bonds in each structure. In the enzyme−substrate complexes (which are the best available models for the transition state), the side chain of E325 makes conserved interactions with O3 and O4 of the ligand (Figure 1b) and the backbone of G307 (not shown) but tends to lose the other contacts. Since the E325A mutant would lack all of these contacts, the more negative $\Delta S^{\ddagger}$ of this mutant relative to WT may indeed result from a less ordered enzyme ground state, to the extent that the apoenzyme structures are

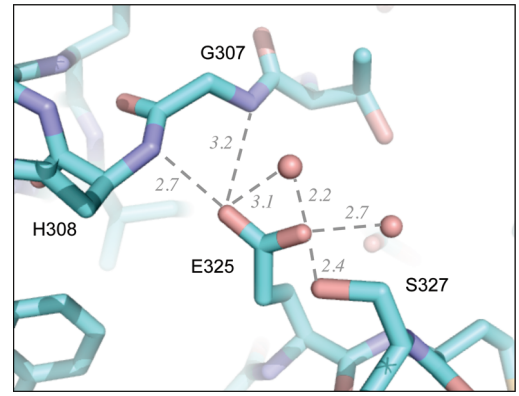

FIGURE 4: Hydrogen bond network of E325 in WT apo-PMM/PGM showing its interactions with the backbone, side chain, and waters. Numbers in italics are hydrogen bond lengths. Although the side chain conformation and details of the network vary in other PMM/PGM structures, contacts with S327 and the two waters are highly conserved in structures of the apoenzyme (1K35 and 1K2Y).

indicative of the ensemble of conformations that likely comprise the ground state of the enzyme in solution. The relative contributions of these different contacts to changes in $\Delta S^{\ddagger}$ are unknown but may include the loss of the backbone contacts that may act to link different segments of the polypeptide chain, as well as the release of one or two water molecules.

The catalytic impairment of the Y17A mutant, in contrast, is mainly determined by the significantly less favorable $\Delta H^{\ddagger}$, compared with WT PMM/PGM, which outweighs the positive change observed in $\Delta S^{\ddagger}$. In fact, if taken at face value, the more positive value for $\Delta S^{\ddagger}$ in the Y17A mutant indicates a less ordered transition state than ground state in this mutant. This somewhat surprising result can perhaps be rationalized because of the unique structural role of Y17 (Figure 1B). Without the critical contacts from this residue, it can be envisioned that the mutant is much less likely to adopt the precise conformation required for high-affinity substrate binding and efficient catalysis, thus impeding the entropically unfavorable but required conformational change

during the WT reaction. In the apoenzyme structures of PMM/PGM, the side chain of Y17A does not participate in any interactions of any type (data not shown), and thus, its absence may be expected to have little effect on the ground state of the reaction, given the caveat noted above.

In addition to conformational change, another major entropy contributor in enzymatic reactions is ion pair desolvation, which relies on electrostatic interactions to stabilize the enzyme−substrate complex. As this potential solvent effect is difficult to address experimentally, we cannot rule out the possibility that it may contribute significantly to the observed thermodynamic changes in the hinge or active site mutants.

Although additional studies, particularly of protein dynamics, are needed to fully investigate the issues raised herein, the kinetic and thermodynamic parameters for the hinge and active site mutants of PMM/PGM described here suggest a broad role for the hinge region in either promoting or sustaining the conformational change required for catalysis. A picture emerges in which the magnitude or rate (or both) of the interdomain rotation of PMM/PGM is influenced by multiple structural features (polypeptide flexibility or rigidity) and interactions (hydrogen bonding networks) in the hinge region. For example, in the case of the conserved proline (P368), the backbone rigidity of this residue could be required to effectively propagate the conformational changes that occur upon substrate binding to the rest of domain 4, and consequently to the active site.

The model described above is consistent with data from other systems, showing that structural rigidity in protein hinges is important for productive conformational changes, recently demonstrated, for example, by detailed studies of TIM dynamics (*16*). Our results further suggest that this may be true regardless of whether the conformational change involves a short 10-amino acid loop (as in TIM) or an entire domain (like the 95-amino acid domain 4 of PMM/PGM). Although derived from different analyses, the similar model resulting from these two disparate systems is thought-provoking in light of theoretical studies that predict enhanced transition rates between conformational states when hinges of intermediate stiffness are utilized (*37*). Such hinges are also least sensitive to the size of the rotating body, which, in the case of PMM/PGM, is an entire domain of the enzyme. Characterization of additional enzyme systems should help determine whether, as the data seem to indicate, the flexibility of protein hinges has evolved to tune and optimize the rates and/or magnitude of conformational change and thereby catalysis.

ACKNOWLEDGMENT

We thank Jay Nix of beamline 4.2.2 at the Advanced Light Source of Lawrence Berkeley National Laboratory for assistance with data collection.

SUPPORTING INFORMATION AVAILABLE

Supporting data (supplementary Figures 1−3 and Table 1) described in the text. This material is available free of charge via the Internet at http://pubs.acs.org.

REFERENCES

1. Olvera, C., Goldberg, J. B., Sanchez, R., and Soberon-Chavez, G. (1999) The *Pseudomonas aeruginosa* algC gene product participates in rhamnolipid biosynthesis. *FEMS Microbiol. Lett. 179*, 85–90.
2. Ye, R. W., Zielinski, N. A., and Chakrabarty, A. M. (1994) Purification and characterization of phosphomannomutase/phosphoglucomutase from *Pseudomonas aeruginosa* involved in biosynthesis of both alginate and lipopolysaccharide. *J. Bacteriol. 176*, 4851–4857.
3. Goldberg, J. B., Coyne, M. J., Jr., Neely, A. N., and Holder, I. A. (1995) Avirulence of a *Pseudomonas aeruginosa* algC mutant in a burned-mouse model of infection. *Infect. Immun. 63*, 4166–4169.
4. Tang, H. B., DiMango, E., Bryan, R., Gambello, M., Iglewski, B. H., Goldberg, J. B., and Prince, A. (1996) Contribution of specific *Pseudomonas aeruginosa* virulence factors to pathogenesis of pneumonia in a neonatal mouse model of infection. *Infect. Immun. 64*, 37–43.
5. Zielinski, N. A., Chakrabarty, A. M., and Berry, A. (1991) Characterization and regulation of the *Pseudomonas aeruginosa* algC gene encoding phosphomannomutase. *J. Biol. Chem. 266*, 9754–9763.
6. Naught, L. E., and Tipton, P. A. (2001) Kinetic Mechanism and pH Dependence of the Kinetic Parameters of *Pseudomonas aeruginosa* Phosphomannomutase/Phosphoglucomutase. *Arch. Biochem. Biophys. 396*, 111–118.
7. Naught, L. E., and Tipton, P. A. (2005) Formation and reorientation of glucose 1,6-bisphosphate in the PMM/PGM reaction: Transient-state kinetic studies. *Biochemistry 44*, 6831–6836.
8. Regni, C., Naught, L. E., Tipton, P. A., and Beamer, L. J. (2004) Structural basis of diverse substrate recognition by the enzyme PMM/PGM from *P. aeruginosa*. *Structure 12*, 55–63.
9. Regni, C., Schramm, A. M., and Beamer, L. J. (2006) The Reaction of Phosphohexomutase from *Pseudomonas aeruginosa*: Structural Insights into a Simple Processive Enzyme. *J. Biol. Chem. 281*, 15564–15571.
10. Regni, C., Tipton, P. A., and Beamer, L. J. (2002) Crystal structure of PMM/PGM: An enzyme in the biosynthetic pathway of *P. aeruginosa* virulence factors. *Structure 10*, 269–279.
11. Henzler-Wildman, K. A., Lei, M., Thai, V., Kerns, S. J., Karplus, M., and Kern, D. (2007) A hierarchy of timescales in protein dynamics is linked to enzyme catalysis. *Nature 450*, 913–916.
12. Cameron, C. E., and Benkovic, S. J. (1997) Evidence for a functional role of the dynamics of glycine-121 of *Escherichia coli* dihydrofolate reductase obtained from kinetic analysis of a site-directed mutant. *Biochemistry 36*, 15792–15800.
13. Bourque, J. R., and Bearne, S. L. (2008) Mutational analysis of the active site flap (20s loop) of mandelate racemase. *Biochemistry 47*, 566–578.
14. Taylor, J. C., Takusagawa, F., and Markham, G. D. (2002) The active site loop of S-adenosylmethionine synthetase modulates catalytic efficiency. *Biochemistry 41*, 9358–9369.
15. Berlow, R. B., Igumenova, T. I., and Loria, J. P. (2007) Value of a hydrogen bond in triosephosphate isomerase loop motion. *Biochemistry 46*, 6001–6010.
16. Kempf, J. G., Jung, J. Y., Ragain, C., Sampson, N. S., and Loria, J. P. (2007) Dynamic requirements for a functional protein hinge. *J. Mol. Biol. 368*, 131–149.
17. Kursula, I., Salin, M., Sun, J., Norledge, B. V., Haapalainen, A. M., Sampson, N. S., and Wierenga, R. K. (2004) Understanding protein lids: Structural analysis of active hinge mutants in triosephosphate isomerase. *Protein Eng., Des. Sel. 17*, 375–382.
18. Rozovsky, S., Jogl, G., Tong, L., and McDermott, A. E. (2001) Solution-state NMR investigations of triosephosphate isomerase active site loop motion: Ligand release in relation to active site loop dynamics. *J. Mol. Biol. 310*, 271–280.
19. Rozovsky, S., and McDermott, A. E. (2001) The time scale of the catalytic loop motion in triosephosphate isomerase. *J. Mol. Biol. 310*, 259–270.
20. Xiang, J., Jung, J. Y., and Sampson, N. S. (2004) Entropy effects on protein hinges: The reaction catalyzed by triosephosphate isomerase. *Biochemistry 43*, 11436–11445.
21. Xiang, J., Sun, J., and Sampson, N. S. (2001) The importance of hinge sequence for loop function and catalytic activity in the reaction catalyzed by triosephosphate isomerase. *J. Mol. Biol. 307*, 1103–1112.

22. Naught, L. E., Regni, C., Beamer, L. J., and Tipton, P. A. (2003) Roles of active site residues in *P. aeruginosa* phosphomannomutase/phosphoglucomutase. *Biochemistry 42*, 9946–9951.
23. Winzor, D. J., and Jackson, C. M. (2005) Interpretation of the temperature dependence of rate constants in biosensor studies. *Anal. Biochem. 337*, 289–293.
24. Winzor, D. J., and Jackson, C. M. (2006) Interpretation of the temperature dependence of equilibrium and rate constants. *J. Mol. Recognit. 19*, 389–407.
25. Regni, C. A., Tipton, P. A., and Beamer, L. J. (2000) Crystallization and initial crystallographic analysis of phosphomannomutase/phosphoglucomutase from *Pseudomonas aeruginosa*. *Acta Crystallogr. D56*, 761–762.
26. Otwinowski, Z., and Minor, W. (1997) Processing of X-ray diffraction data collected in oscillation mode. *Methods Enzymol. 276*, 307–326.
27. Pflugrath, J. W. (1999) The finer things in X-ray diffraction data collection. *Acta Crystallogr. D55*, 1718–1725.
28. Murshudov, G. N., Vagin, A. A., Lebedev, A., Wilson, K. S., and Dodson, E. J. (1999) Efficient anisotropic refinement of macromolecular structures using FFT. *Acta Crystallogr. D55*, 247–255.
29. Emsley, P., and Cowtan, K. (2004) Coot: Model-building tools for molecular graphics. *Acta Crystallogr. D60*, 2126–2132.
30. Hubbard, S. J., and Thornton, J. M. (1993) *NACCESS*, Department of Biochemistry and Molecular Biology, University College London, London.
31. Jones, S., and Thornton, J. M. (1996) Principles of protein-protein interactions. *Proc. Natl. Acad. Sci. U.S.A. 93*, 13–20.
32. Maiti, R., Van Domselaar, G. H., Zhang, H., and Wishart, D. S. (2004) SuperPose: A simple server for sophisticated structural superposition. *Nucleic Acids Res. 32*, W590–594.
33. DeLano, W. L. (2002) *The PyMOL Molecular Graphics System*, DeLano Scientific, San Carlos, CA.
34. Thompson, J. D., Higgins, D. G., and Gibson, T. J. (1994) CLUSTAL W: Improving the sensitivity of progressive multiple sequence alignment through sequence weighting, position-specific gap penalties and weight matrix choice. *Nucleic Acids Res. 22*, 4673–4680.
35. Clamp, M., Cuff, J., Searle, S. M., and Barton, G. J. (2004) The Jalview Java alignment editor. *Bioinformatics 20*, 426–427.
36. Regni, C., Shackelford, G. S., and Beamer, L. J. (2006) Complexes of the enzyme phosphomannomutase/phosphoglucomutase with a slow substrate and an inhibitor. *Acta Crystallogr. F62*, 722–726.
37. Neher, R. A., Mobius, W., Frey, E., and Gerland, U. (2007) Optimal flexibility for conformational transitions in macromolecules. *Phys. Rev. Lett. 99*, 178101.

BI8005219